

# Temperatures of EUV-Emitting Plasma Structures Observed by the *Transition Region And Coronal Explorer*

Jongchul Chae<sup>1</sup> and Young-Deuk Park<sup>2</sup>, Yong-Jae Moon<sup>2,3</sup>, Haimin Wang<sup>3</sup>, H. S. Yun<sup>4</sup>

## ABSTRACT

The *Transition Region And Coronal Explorer* has revealed various kinds of EUV-emitting plasma structures in the solar upper atmosphere in unprecedented details. The filter ratio  $195\text{\AA}/171\text{\AA}$  has been conventionally used to determine the plasma temperatures, but this method has a shortcoming that it may not yield a unique value of temperature for a given ratio. Therefore, we introduce a new method employing two filter ratios ( $195\text{\AA}/171\text{\AA}$  and  $284\text{\AA}/195\text{\AA}$ ). It is demonstrated that this color-color method is effective in unambiguous determination of plasma temperatures in a wide range. We have obtained a temperature of  $1 \times 10^6$  K for a loop that is bright in  $171\text{\AA}$ , but hardly visible in  $284\text{\AA}$ ; a higher temperature of  $2 \times 10^6$  K for a loop that is well visible in  $195\text{\AA}$  and  $284\text{\AA}$ , but not in  $171\text{\AA}$ ; and a transition region temperature of  $2.5 \times 10^5$  K for a low-lying loop that is well visible in all the EUV wavelengths. In addition, we have found that ‘moss’ structures have temperatures around  $1 \times 10^6$  K and EUV jets have temperatures of about  $2.5 \times 10^5$  K.

*Subject headings:* Sun: EUV radiation — Sun: transition region — Sun: corona

## 1. INTRODUCTION

The *Transition Region And Coronal Explorer* (*TRACE*, Handy et al. 1999; Schrijver et al. 1999) has observed the sun in unprecedented details at extreme-ultraviolet (EUV)

---

<sup>1</sup>Department of Astronomy and Space Science, Chungnam National University, Daejeon 305-764, Korea; [chae@cnu.ac.kr](mailto:chae@cnu.ac.kr)

<sup>2</sup>Korea Astronomy Observatory, Daejeon, 305-348, Korea

<sup>3</sup>Big Bear Solar Observatory, NJIT, 40386 North Shore Lane, Big Bear City, CA 92314

<sup>4</sup>Astronomy Programs, SEES, Seoul National University, Seoul 151-742, Korea

wavelengths in the three EUV passbands around 171 Å, 195 Å, and 284 Å. Since these filters are most sensitive to EUV emissions from plasmas of coronal temperatures 1 MK, 1.5 MK, and 2 MK, respectively, it is customary to choose 1-2 MK temperatures for EUV-emitting plasmas. The precise determination of temperature in this range has often been done based on the filter ratio 195/171 as shown in Figure 1. Note this ratio is very sensitive to temperature variation around 1 MK. Unfortunately, however, it may not yield a unique value of temperature for a given ratio. For example, the 195/171 value of about 0.2 may represent either a coronal temperature of 1 MK or a transition region temperature of about 0.3 MK. Usually the coronal temperature is selected, mainly because the sensitivity of the 171 filter (or 195 filter) has a peak at a coronal temperature. But it should be recalled that transition region plasmas are usually denser than coronal plasmas so that the response reduction (by a factor of 10 in this example) is easily compensated for with a moderate density increase (by a factor 3.1 in this example). Therefore, it appears crucial to have an objective way of resolving between the coronal temperatures and the transition region temperatures for the measurements of temperatures, emission measures and densities of EUV-emitting plasmas without pitfalls.

In the present Letter, we introduce a new method employing the two filter ratios (195/171 and 284/195). We have found that including the 284 filter serves the purpose of resolving ambiguity between plasma temperatures at different regimes.

## 2. METHOD

The principle is simple. Suppose all the EUV emissions at the three wavelengths originate from the same volume filled with isothermal plasma with temperature  $T$ . Then the light intensity at each band is given by  $I_k = G_k(T, A) \cdot \text{EM}$  where the subscript  $k$  denotes either of the wavelengths, and  $G_k$ , its temperature response. Here  $A$  represents the abundances of emitting elements. Since the emission measure EM is independent of wavelength, it follows  $C_1 \equiv \log(I_{284}/I_{195}) = \log(G_{284}/G_{195})$  and  $C_2 \equiv \log(I_{195}/I_{171}) = \log(G_{195}/G_{171})$ . Note both  $C_1$  and  $C_2$  are now functions of temperature and element abundances. Given element abundances, the set of all the points  $(C_1, C_2)$  constitutes a curve on the  $X - Y$  plane, a point on which corresponds to a unique temperature. Therefore, the pair of the observed  $C_1$  and  $C_2$  can be used in principle to uniquely determine the temperature of EUV-emitting plasma without ambiguity.

Figure 2 shows the theoretical curves of  $(C_1, C_2)$  produced based on the temperature responses given by the standard *TRACE* procedure `trace.t_resp.pro` (Aschwanden et al. 2000a), one with the photospheric abundance (Grevesse & Sauval 1998) and the other with

coronal abundance (Feldman 1992). Note the curves have two-fold shapes, with the inner portions of transition region temperatures and the outer portions of coronal temperatures. The major difference between the two curves is found in the temperature range  $10^{5.4}$  to  $10^{5.8}$  K. At other temperatures, the difference is small compared with the observational errors to be explained below.

Note that according to the curve with the coronal abundance, two different temperatures, for example,  $10^{5.5}$  K and  $10^6$  K have the same value  $C_2 \equiv \log(I_{195}/I_{171}) = -0.65$ . Therefore, using the ratio 195/171 only can not determine the temperature without ambiguity. But these temperatures correspond to different values of  $C_1 \equiv \log(I_{284}/I_{195}) = -0.65$  and  $-1.15$ , respectively. Therefore, the newly introduced filter ratio  $C_1$  makes it possible to discriminate between the two temperature regimes.

For actual measurements of the filter ratios, it is important to keep in mind that the observed specific intensity of a plasma structure  $I_{obs,k}$  at the  $k$  passband contains not only its own emission  $I_k$ , but also the emission from its background  $I_{bg,k}$  and foreground plasma  $I_{fg,k}$ , so that  $I_{obs,k}(x, y) = I_k(x, y) + I_{bg,k}(x, y) + I_{fg,k}(x, y)$ . Here  $(x, y)$  denotes the position on the image plane. If the EUV emitting structure is embedded in the diffuse background and foreground plasma, then we have  $I_{bg,k}(x, y) + I_{fg,k}(x, y) \approx I_{bg,k}(x_0, y_0) + I_{fg,k}(x_0, y_0) \approx I_{obs,k}(x_0, y_0) \equiv I_{ref,k}$  with a chosen reference point  $(x_0, y_0)$  in the neighborhood of  $(x, y)$ . Thus it follows  $I_k(x, y) \approx I_{obs,k}(x, y) - I_{ref,k}$  to a good approximation. For practical implementation, we set  $I_{ref,k}$  equal to the mean of  $I_{obs,k}$  over the  $3 \times 3$  pixels centered on  $(x_0, y_0)$  to reduce the uncertainty in  $I_{ref,k}$  due to noise. Moreover, to avoid the unrealistic measurement of negative  $I_k(x, y)$  due to noise, we force  $I_k(x, y)$  to be greater than or equal to the standard deviation of  $I_{obs,k}$  over the  $3 \times 3$  pixels centered on  $(x, y)$ . We then calculate the logarithmic filter ratios  $C_1$  and  $C_2$  at every point of the  $3 \times 3$  pixels centered on  $(x, y)$ , and take their mean values as the final measurements and their standard deviations as the estimated errors.

In reality, the observed colors may be rather sensitive to the choice of the reference point, because the EUV emitting plasmas around the measurement point are highly structured at small scales, rather than being uniform. To minimize the effect of such non-uniformity, we select a reference point that is as close to the EUV emitting structure of our interest as possible, but is not a part of it. As a result, the distance between the measurement point and the reference point may be as small as the width of the EUV emitting structure, typically being a few arc seconds. Even with such care, the dependence of the observed colors on the chosen reference point may be a significant source of errors in some cases. Our experience suggests the unavoidable arbitrariness of selecting the reference point may result in the errors of  $\Delta C_1 = \Delta C_2 = 0.1 \sim 0.2$ , where the errors are big when the brightness contrasts between the measurement point and the reference point are small.

It should be noted that measuring filter ratios requires the simultaneity of the images taken at different passbands. TRACE images at different pass bands are taken successively, and it may take a few tens of seconds or longer to get a set of EUV images at the three passbands. Thus, the simultaneity is not guaranteed when rapidly evolving EUV structures are observed. In this case, a special treatment like interpolation would be required to ensure the simultaneity that is essential for the precise measurement of temperature. In the present work, we do not attempt to such treatment, but instead provide an estimate of probable errors. In the case of long-lived EUV emitting structures like loops, the delayed times between different filter images do not become a problem.

### 3. RESULTS

The centers of the ellipses in Figure 2 represent the mean values of  $C_1$  and  $C_2$  at several EUV-emitting plasma structures, and their  $x$  and  $y$  radii represent the estimated errors in  $C_1$  and  $C_2$ . Figure 2 shows that for the temperatures of the EUV-emitting plasma structures, the color-color method is nearly independent of the employed abundance. Figure 3 compares the images of these structures seen at the three passbands, which are discussed below in detail.

**(a) 171/195 loop** This loop is very bright at 171. It is also well visible at 195, even though its intensity significantly drops. At 284, it is hardly visible. This emission characteristic is quantitatively expressed in the values  $C_1 = -1.4$  and  $C_2 = -0.6$ . Our method indicates that these values are fairly consistent with the EUV emission from plasma with a temperature of about  $10^{6.0}$  K (see the + symbol in Figure 2). Figure 3 implies that the loop must be very big since only a small portion near its footpoint is covered in the field of view. It is now well-known from TRACE observations that this kind of 1 MK loops usually surround the hotter X-ray coronal loops (Schrijver et al. 1999). Since these loops are most prominent in the EUV wavelengths, especially at 171, their thermodynamic properties have been extensively studied based on TRACE observations by Lenz et al. (1999a, b) and Aschwanden, Nightingale & Alexander (2000b). The conventional 195/171 filter ratio method with a 1 MK solution works very well in these loops.

**(b) 195/284 loop** This loop is well visible at 195 and 284, but is hardly visible in 171. This loop is smaller than the 171 loop in (a). Figure 2 shows that there is an uncertainty in determining  $C_2$  (asterisk symbol), mainly because of the difficulty in measuring the 171 intensity. Nevertheless, it is not difficult to draw the conclusion that  $T \approx 10^{6.3}$  K in this loop. This indicates that this loop is hotter than the 171/195 loop in (a), and represents the

inner hot shell of the active region. This kind of 2 MK loops have rarely been studied based on *TRACE* observations. The present result suggests the good possibility of investigating 2 MK loops using *TRACE* data.

**(c) 171/195/284 loop** This loop is clearly visible at all the wavelengths. Figure 2 shows that this loop has a temperature of about  $10^{5.38}$  K (diamond). Therefore, this loop is a loop at transition region temperatures, being distinct from the 1 MK 171/195 loop in (a) and 2 MK 195/284 loop in (b). This loop is a clear example showing that not all the TRACE/EUV loops have coronal temperatures. This kind of loops are often found in filaments being mingled with  $H\alpha$  loops or EUV absorption features (see, for example, Figure 2 of Chae 2000). Note loops having transition region temperatures have been reported many times from the *SOHO*/CDS observations (see Brekke 1999 for a review) or *SOHO*/SUMER observations (e.g., Chae et al. 2000).

**(d) moss** This finely textured, low-lying bright emission commonly called “moss” (Berger et al. 1999a, b) is most prominently seen at 171. The 284 emission is less conspicuous than the 171 emission, possibly because most of the 284 emission may be from the foreground hotter diffuse plasma. The choice of the reference point as indicated by the cross mark, produces the filter ratios indicating that it has a temperature of about  $10^{6.03}$  K (triangle in Figure 2). This value is compatible with the temperature range of 0.6 to 1.5 MK obtained from the *SOHO*/CDS observations (Fletcher & De Pontieu 1999). Moss is believed to represent the cooler base of hot loops  $T > 2$  MK (Berger et al. 1999a, b; Fletcher & De Pontieu 1999; Martens, Kankelborg & Berger 2000).

But it appears that the filter ratios obtained for the moss may be sensitive to the chosen reference point. We have found that, for instance, if a point at the nearby darker region is selected as the reference, the 284 and 195 intensities increases and the colors indicates a temperature may be about  $10^{5.4}$  K, which is much different from  $10^{6.03}$  K. The difficulty of choosing a non-arbitrary reference point seems to arise from the fact the EUV emission in the moss is highly structured — horizontally and vertically, and rapidly varies in time. A very careful treatment of data would be required for a solid determination of temperatures in moss.

**(e) EUV jet** EUV-emitting plasma jets were observed by *TRACE* (Chae et al. 1999; Alexander & Fletcher 1999). These observations showed that *TRACE* EUV jets are similar to *Yohkoh* X-ray jets in shape and velocity, but are smaller and shorter-lived than X-ray jets. For this reason, Chae et al. (1999) conjectured that EUV jets may represent the small-

scale extension of X-ray jets. So far, their temperatures have not been carefully measured from *TRACE* data, but they are often assumed to be about 1 MK (e.g., Alexander & Fletcher 1999). Our application of the two-filter-ratio method, however, shows that they have transition temperatures around  $10^{5.35}$  K (square in Figure 2), not around 1 MK. This unambiguous determination is possible with the help of 284 data. If the jet has 1 MK temperature, it would appear as faint structures. But as shown in Figure 3, the jet is well visible at all the wavelengths, like the 171/195/284 loop in (c). Note that there is about 50 s time difference between the EUV images, with the longest exposure of 25 s was taken for the 284 image. Since the jet is moving and brightness at each point is changing, the time difference may be a cause of uncertainty in determining filter ratios. By comparing the colors with those determined from another set of images taken close in time for the same jet, we roughly estimate the uncertainties in  $C_1$  and  $C_2$  to be about 0.2. These errors correspond to  $\Delta \log T \leq 0.1$ , which is tolerable for our purpose.

It is rather surprising that *TRACE* EUV jets have transition region temperatures. This result suggests that EUV jets may be more relevant to other diverse jet-like phenomena observed at transition region temperatures (see Brekke 1999) than to much hotter X-ray jets.

#### 4. DISCUSSION

For unambiguous determination of temperatures of EUV-emitting plasmas observed by *TRACE*, we have developed a new method employing two filter ratios (195Å/171Å, 284Å/195Å). By applying this color-color method, we have determined the temperatures of the five selected plasma structures: (a) 171/195 loop, (b) 195/284 loop, (c) 171/195/284 loop, (d) moss and (e) EUV jet. The result is summarized in Table 1, which also compares the different kinds of filter ratio method. Note that there are at least three groups of plasma structures having different temperature regimes and showing different EUV emission characteristics. One is 1 MK plasma structures (a) and (d) that are usually very bright at 171, and are well visible at 195, but are hardly visible at 284. Another is hotter 2 MK plasma structures (b) that are well visible at 195 and 284, but not at 171. The last is 0.2 to 0.3 MK transition region plasma structures (c) and (e) that are well visible at all the wavelengths. There may be additional groups that have temperature regimes much different from these. Warren et al. (1999) clearly demonstrated that 10 MK flare plasma may also significantly contribute to *TRACE* EUV emission.

Like the conventional filter ratio method, our method basically assumes that EUV-emitting plasma structures are isothermal, each being characterized by a single tempera-

ture. Observations, however, support that each EUV or X-ray emitting plasma structure may consist of many, fine-scale components with different temperatures (e.g., Alexander & Fletcher 1999; Aschwanden et al. 2000b; Gary et al. 1996). An ideal way of describing multi-temperature plasma would be to specify the differential emission measure (DEM) as a function of  $T$  (e.g, Fletcher & De Pontieu 1999 ), which can be hardly realized in *TRACE* observations. Alternatively, a single temperature obtained from *TRACE* data by applying our method may be interpreted as an average of  $T$  that is weighted by DEM and filter responses. Obviously, if the observed plasma structure is far from being isothermal, our method will break, and the observed colors ( $C_1$ ,  $C_2$ ) may be expressed as a point in Figure 2 that deviate much from the theoretical curve. The observed closeness between the data points and the theoretical curve as shown in Figure 2 suggests that the isothermal assumption may be good enough for the EUV-emitting plasma structures examined in the present work.

We would like to thank the referee for the constructive comments. We greatly appreciate the open data policy of the *TRACE* team. This work was supported by Korea Research Foundation Grant (KRF-2001-015-DP0617), the National Research Laboratory project (code no: M10104000059-01J000002500), BK21 project of the Korean Government, and NASA (grant NAG5-10894).

## REFERENCES

- Alexander, D. & Fletcher, L. 1999, *Sol. Phys.*, 190, 167
- Aschwanden, M. J., Tarbell, T. D., Nightingale, R. W., Schrijver, C. J., Title, A., Kankelborg, C. C., Martens, P., & Warren, H. P. 2000a, *ApJ*, 535, 1047
- Aschwanden, M. J., Nightingale, R. W., & Alexander, D. 2000b, *ApJ*, 541, 1059
- Berger, T. E., de Pontieu, B., Schrijver, C. J., & Title, A. M. 1999a, *ApJ*, 519, L97
- Berger, T. E., De Pontieu, B., Fletcher, L., Schrijver, C. J., Tarbell, T. D., & Title, A. M. 1999b, *Sol. Phys.*, 190, 409
- Brekke, P. ;. 1999, *Sol. Phys.*, 190, 379
- Chae, J., Qiu, J., Wang, H., & Goode, P. R. 1999, *ApJ*, 513, L75
- Chae, J., Wang, H., Qiu, J., Goode, P. R., & Wilhelm, K. 2000, *ApJ*, 533, 535
- Chae, J. 2000, *ApJ*, 540, L115

- Feldman, U. 1992, *Phys. Scr*, 46, 202
- Fletcher, L. & de Pontieu, B. 1999, *ApJ*, 520, L135
- Gary, D. E., Wang, H., Nitta, N., & Kosugi, T. 1996, *ApJ*, 464, 965
- Grevesse, N. & Sauval, A. J. 1998, *Space Science Reviews*, 85, 161
- Handy, B. N. et al. 1999, *Sol. Phys.*, 187, 229
- Lenz, D. D., DeLuca, E. E., Golub, L., Rosner, R., & Bookbinder, J. A. 1999a, *ApJ*, 517, L155
- Lenz, D. D., DeLuca, E. E., Golub, L., Rosner, R., Bookbinder, J. A., Litwin, C., Reale, F., & Peres, G. 1999b, *Sol. Phys.*, 190, 131
- Martens, P. C. H., Kankelborg, C. C., & Berger, T. E. 2000, *ApJ*, 537, 471
- Schrijver, C. J. et al. 1999, *Sol. Phys.*, 187, 261
- Warren, H. P., Bookbinder, J. A., Forbes, T. G., Golub, L., Hudson, H. S., Reeves, K., & Warshall, A. 1999, *ApJ*, 527, L121

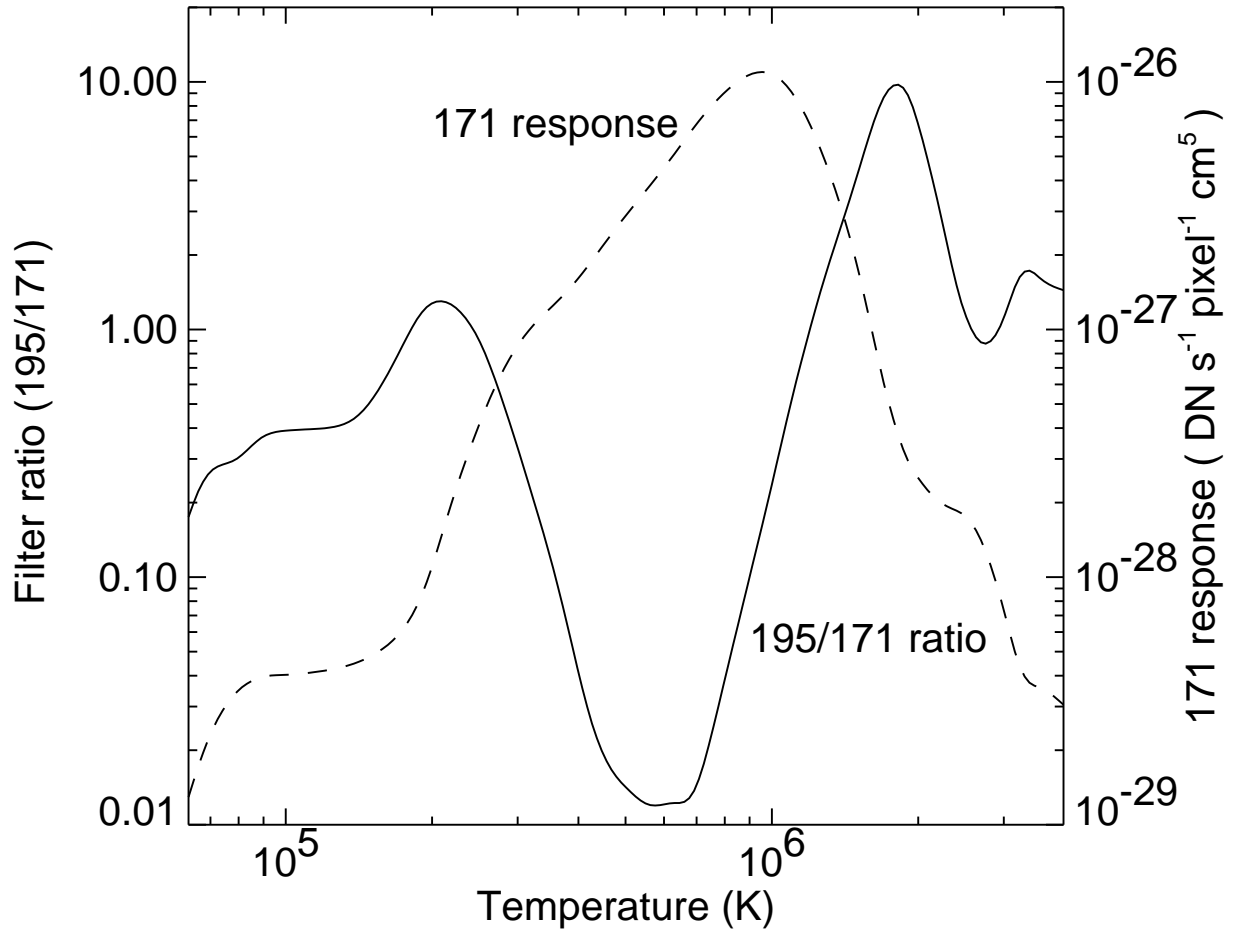


Fig. 1.— The 171 filter response (---) and the filter ratio 195/171 (—) as functions of plasma temperature assuming the Feldman coronal abundance.

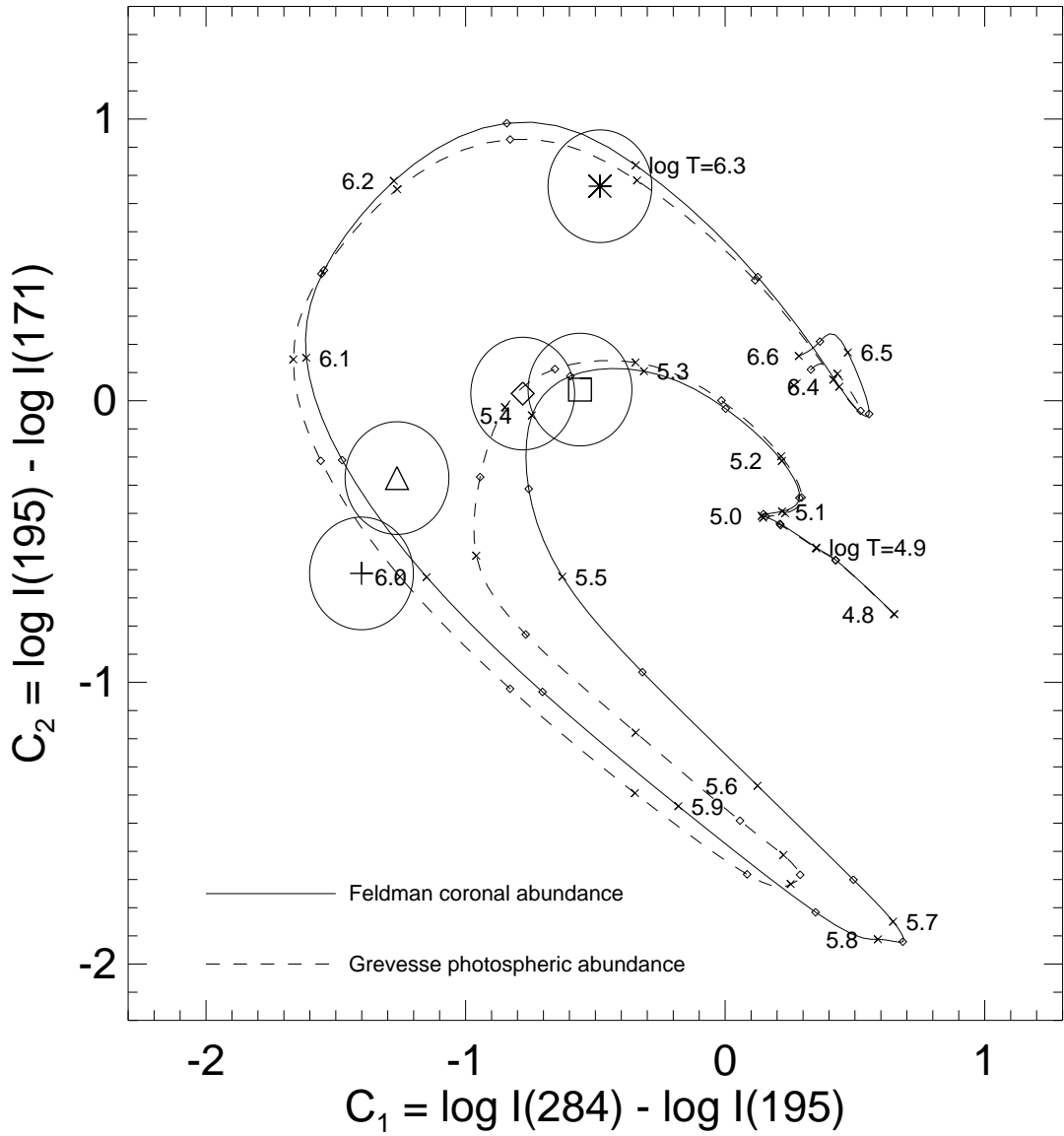


Fig. 2.— The color-color diagram for different plasma structures (a) 171/195 loop (+), (b) 195/284 loop (asterisk), (c) 171/195/284 loop (diamond), (d) moss (triangle), and (e) EUV jet (square).

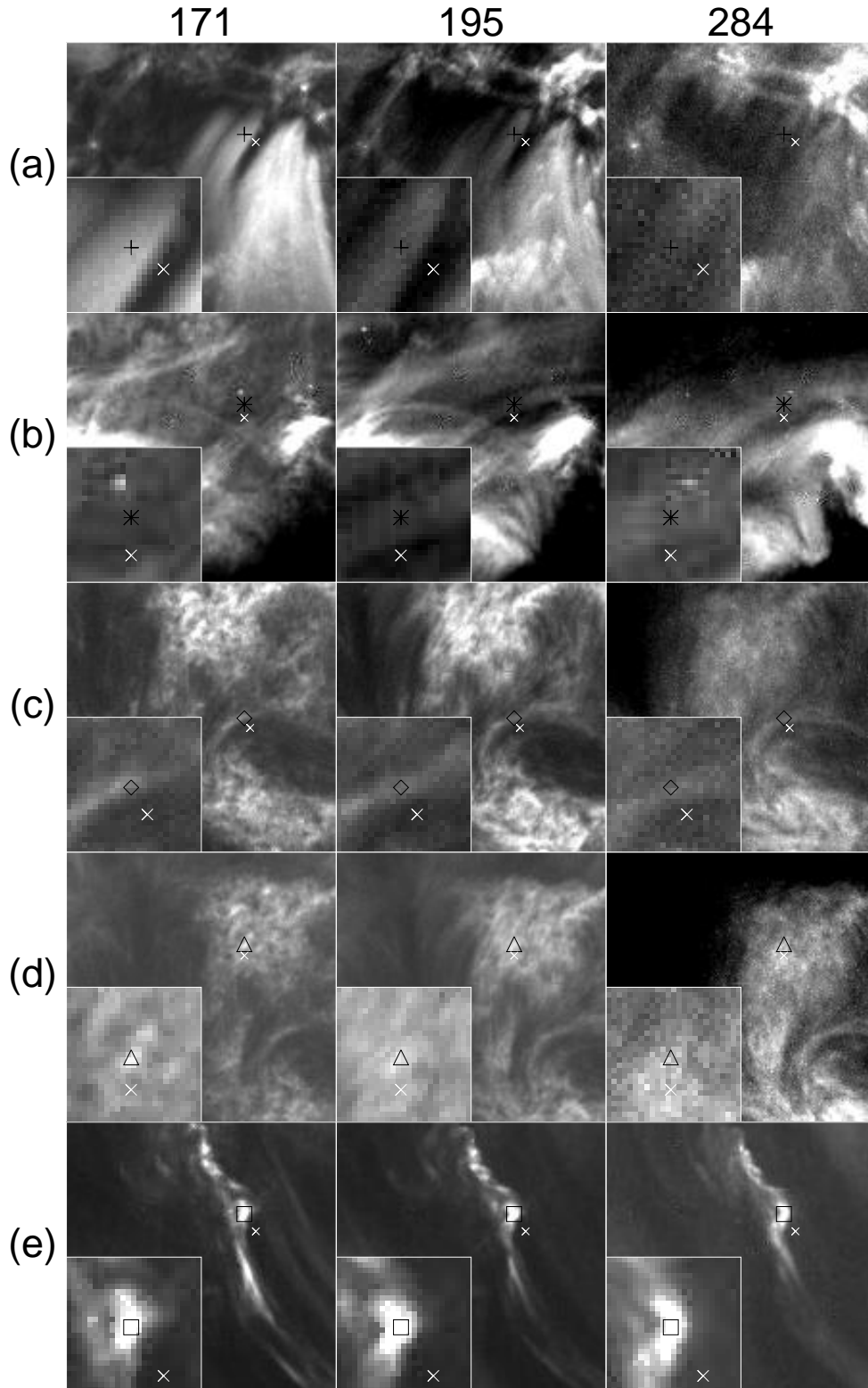


Fig. 3.— Different kinds of EUV-emitting plasma structures with different temperatures: (a) a 171/195 loop ( $1.0 \times 10^6$  K), (b) a 195/284 loop ( $2.0 \times 10^6$  K), (c) a 171/195/284 loop ( $2.4 \times 10^5$  K), (d) moss ( $1.1 \times 10^6$  K), and (e) an EUV jet ( $2.5 \times 10^5$  K). The bigger field of view in all the cases is  $70''$  by  $70''$ , and the enlarged smaller field of view is  $12''$  by  $12''$ . The black symbol in each image refers to the point of measurement and the smaller, white symbol, to the reference point.

Table 1: Determination of temperatures of EUV-emitting structures using different filter ratio methods.

Structure	Ratio 195/171	Ratio 284/195	Two ratios
171/195 loop	1.0 MK	not good <sup>a</sup>	1.0 MK
195/284 loop	not good <sup>a</sup>	1.9 MK	2.0 MK
171/195/284 loop	1.2 MK	1.8 MK	.24 MK
Moss	1.1 MK	not good <sup>a</sup>	1.1 MK
EUV jet	1.2 MK	1.9 MK	0.25 MK

---

<sup>a</sup>The single ratio method is not good in that the intensity in one filter is so weak and the ratio is poorly determined.